

Modeling and Analysis of Hydrogen Atoms

Anders Østergaard Madsen

Abstract Hydrogen atoms are elusive seen from the point of view of the X-ray crystallographer. But they are also extremely important, being involved in a wealth of intermolecular interactions and thereby defining the way molecules interact. Most experimental charge density studies are performed on compounds containing hydrogen, yet a commonly accepted strategy to deal with these elusive but so important atoms is only just about to surface. We review the efforts to determine a strategy for the modeling of hydrogen atoms, as well as a number of recent studies where the modeling of hydrogen atoms has had a major impact on the chemical conclusions drawn from analysis of the experimental charge densities.

Keywords Charge density analysis · Debye–Waller factors · Hydrogen atoms

Contents

1	Introduction	22
2	Bias in Static Charge-Density Models Due to Incorrect Deconvolution of Thermal Motion and Incorrect Nuclear Positions of Hydrogen Atoms	23
2.1	Hydrogen Atom Positions	26
2.2	Hydrogen Atom ADPs	26
2.3	A Comment on Using the Residual Density and R-Values to Judge the Quality of Models for Hydrogen Atoms	28
3	How to Obtain H Atom Positions and Anisotropic Displacement Parameters	29
3.1	Information from Neutron Diffraction	29
3.2	Estimated Hydrogen Positions	30
3.3	Ab Initio/Hirshfeld Atom Refinement	32

3.4	Estimated H ADPS Based on a Combination of Rigid Body Motion and Internal Motion	32
3.5	Estimates of H ADPs Based Solely on Force-Field or Ab Initio Calculations	38
4	Charge-Density Studies with a Special Focus on H Atoms	39
4.1	Strong Hydrogen Bonds	40
4.2	EFGs at the H Nuclei	41
4.3	Molecular Interactions	42
5	Outlook	47
	References	48

Abbreviations

ADP	Anisotropic displacement parameter
BCP	Bond critical point
DFT	Density functional theory
HF	Hartree–Fock
IAM	Independent atom model
MSD	Mean square displacement
PES	Potential energy surface
SDS	Scattering factor for hydrogen by Stewart, Davidson, and Simpson

1 Introduction

The properties of hydrogen atoms have attracted crystallographers for many years, because of the importance of hydrogen bonding in virtually all areas of organic chemistry and structural biology. Crystallography has played – and continues to play – a major role in defining and elucidating the properties of hydrogen bonding [1].

However, because X-rays interact with the electron density in the crystal, the information about the H atom nuclear position and motion that can be derived from X-ray diffraction analysis is limited; the lack of core-electrons and the diffuse character of the valence shell make the scattering power of hydrogen poor compared to other elements. For this reason, the majority of structural studies of hydrogen bonding in molecular crystals has relied on neutron diffraction, where the scattering length of hydrogen has a magnitude comparable to the heavier elements.

In experimental charge density studies, the combined X-ray and neutron diffraction study has proven to be an important tool to study the charge density of hydrogen atoms. Unfortunately, it is not always possible to perform neutron diffraction experiments; it might be impossible to grow crystals of a sufficient size (larger than 1 mm³), or the researchers' access to a neutron source is limited. Because the speed and quality of the X-ray diffraction experiments have increased tremendously, conducting neutron diffraction experiments have become a bottleneck which may prohibit comparative studies of charge densities in a series of related compounds.

For these reasons, many researchers have avoided the use of neutron diffraction data and limited their model of the hydrogen atom nuclear parameters to an isotropic displacement parameter, combined with a very limited description of the charge density of the hydrogen atoms. In fact, more than 80% of the studies in the period from 1999 to 2007 used this approach [2]. In this chapter, we review the efforts that has been done to elucidate the errors introduced in the charge density models by using a less than adequate description of the hydrogen atoms, as well as a number of methods to obtain a better model of hydrogen atoms, in lieu of neutron diffraction data.

This review is divided into three parts:

1. In Sect. 3, we review the work that demonstrate how an incorrect description of the nuclear parameters of H atoms leads to erroneous models of the static charge density in the crystal.
2. In Sect. 4, we review the efforts to determine the positions and thermal motion of hydrogen atoms for the use in experimental charge-density studies. We briefly describe the pros and cons of using information from neutron diffraction experiments, but focus mainly on presenting methods of estimating hydrogen anisotropic displacement parameters (ADPs) based on the analyses of the thermal motion of the non-hydrogen atoms combined with information about the internal motion of the hydrogen atoms. It is not the purpose of this chapter to compare the accuracy of these different approaches to estimate hydrogen ADPs – that has been done quite thoroughly by Munshi et al. [2].
3. In Sect. 5, we describe recent charge-density studies where the use of accurate information about the H atom position and thermal motion has been crucial, and consider the strengths and weaknesses of the different approaches to estimate the positions and thermal motion of hydrogen atoms.

2 Bias in Static Charge-Density Models Due to Incorrect Deconvolution of Thermal Motion and Incorrect Nuclear Positions of Hydrogen Atoms

Even at the lowest temperatures atoms in crystals are vibrating. The diffracted X-ray or neutron intensities correspond to the diffraction signal of the averaged electron and nuclear density $\langle\rho\rangle$. The brackets denote a double average over the displacement of atoms from their mean positions; a time average over the atomic vibrations in each unit cell, as well as a space average over all unit cells. The structure factor of a reflection \mathbf{h} is given by the Fourier transform of the average density of scattering matter.

$$F(\mathbf{h}) = \int \langle\rho(\mathbf{r})\rangle \exp(2\pi i\mathbf{h} \cdot \mathbf{r})d\mathbf{r}. \quad (1)$$

The standard independent atom model (IAM) used in structural studies, where the atomic scattering factors are spherically symmetric, as well as the multipole model used in charge-density studies is constructed in order to deconvolute the thermal motion from a model of the static electron density. In this approach, the *mean thermal* electron density of an atom is considered to be the convolution of a static density $\rho_k(\mathbf{r})$ with the probability density function (PDF) p_k describing the probability of having atom k displaced from its reference position.

$$\langle \rho_k(\mathbf{r}) \rangle = \int \rho_k(\mathbf{r} - \mathbf{r}_k) p_k(\mathbf{r}_k) d\mathbf{r}_k = \rho_k(\mathbf{r}) \times p_k. \quad (2)$$

The structure factors can then be approximated by a sum over contributions from all N atoms of the unit cell:

$$F(\mathbf{h}) \approx \sum_{k=1}^N n_k f_k(\mathbf{h}) T_k(\mathbf{h}) \exp(2\pi i \mathbf{h} \cdot \mathbf{r}_{k0}), \quad (3)$$

where f_k is the form factor of atom k and $T_k(\mathbf{h})$ is the Fourier transform of the PDF, p_k , describing the displacement of atom k from its reference position \mathbf{r}_{k0} . The atomic form factors are described by the multipole model. The PDF p_k and its Fourier transform $T_k(\mathbf{h})$ – the atomic Debye–Waller factor – are normally described by trivariate Gaussian functions, because it can be shown that the PDF is a Gaussian distribution if the vibrations of the atoms are harmonic [3]. A common way to express the trivariate Gaussian atomic Debye–Waller factor is in the coordinate system of the crystallographic unit cell with axes a^i , $i \in 1, 2, 3$:

$$T_k(\mathbf{h}) = \exp \left(-2\pi^2 \sum_{i=1}^3 \sum_{j=1}^3 h_i a^i U^{ij} a^j h_j \right), \quad (4)$$

with

$$U^{ij} = \langle \Delta \xi^i \Delta \xi^j \rangle, \quad (5)$$

where $\Delta \xi^i$ are the components of the displacement vector \mathbf{u} of atom k from its mean position. The elements U^{ij} of the 3×3 tensor \mathbf{U} are the ADPs, and in this form the elements have dimension (length^2) and can be directly associated with the mean-square displacements of the atom considered in the corresponding directions. There exist a confusing range of different representations and nomenclature of the ADPs – an overview and some recommendations concerning the nomenclature are given by Trueblood et al. [4].

A major goal of experimental charge-density analysis is to ensure that a proper deconvolution of vibration effects and static charge density is obtained. The entire model of $\langle \rho(\mathbf{r}) \rangle$ consisting of both static and dynamic elements is refined against

one set of structure factors, cf. (3). Because the parameters of the multipole model correlate with the parameters describing the positions and mean square displacements of the atoms it is evident that there can be no proper description of the static charge density without a proper description of the positions and molecular motion of the atoms, and vice versa.

One of the advantages of the multipole model is that it provides a much better deconvolution of the thermal motion of non-hydrogen atoms than the IAM model. However, the situation is more complicated for hydrogen atoms. Historically, the scattering factor of hydrogen was based on the *ab initio* wavefunction of an isolated hydrogen atom. The electron density of an isolated H atom is much different from a bonded hydrogen atom, and the scattering factor lead to meaningless bond distances and thermal parameters for hydrogen atoms. The so-called SDS scattering factor based on the *ab initio* electron density of the hydrogen molecule [5] lead to a considerable improvement, and this scattering factor is today the standard in popular structure refinement programs. Even with the SDS scattering factor, covalent bond lengths to hydrogen obtained by refinement against X-ray diffraction data are roughly 20% shorter than the values obtained from refinement against neutron diffraction data. And while the SDS scattering factor allows refinement of isotropic displacement parameters, it is not possible to obtain ADPs that are in agreement with neutron diffraction data, or even physically meaningful.

This review has a special focus on the modeling of the nuclear parameters of the hydrogen atoms, however, a few comments on the modeling of the electron densities are important. Model studies of diatomic hydrides by Chandler and Spackman [6] indicated that in order to model the electron densities of the hydrogen atoms, it is important to require multipole expansions to at least the quadrupole level, with one single-exponential radial function per multipole and all exponents optimized. Numerous experimental studies including a range of the studies reviewed in this chapter indicate that the quadrupole terms are important. The radial functions are usually of the single exponential form, $r^n \exp(-\alpha r)$, with $n = 0, 1, 2$ for the monopole, dipole, and quadrupole terms, respectively. However, optimization of exponents of the radial functions is not conventional, and if performed only with a common exponent α for all the radial functions on all H atoms. This limited refinement of exponents is dictated by the quality and resolution of the experimental data.

Experimental charge densities can also be studied using maximum entropy methods. Some recent developments are described by Netzel et al. [7, 8]. The electron densities obtained by this method are mean thermal charge densities, i.e., there is no attempt to deconvolute dynamic effects from a static electron density model, and thereby one of the major challenges of the multipole model is avoided. The MEM method and the studies of thermally averaged charge densities are very interesting but out of the scope of the present review that deals with the deconvolution of the thermal motion of hydrogen atoms from the thermally averaged charge density.

2.1 *Hydrogen Atom Positions*

As mentioned previously, the standard SDS scattering factor [5] improved the description of the hydrogen atoms tremendously as compared to the scattering factor of an isolated H atom, however it leads to bond lengths that are about 20% too short, as compared to the values obtained from neutron diffraction data. In fact, the SDS scattering factor was designed to obtain the best possible least-squares fit against the diffraction data, and not to obtain the correct position of the hydrogen atom. Since the electron density of a bound hydrogen atom is polarized toward the bonding atom, it is difficult to obtain a better estimate of the hydrogen position with a spherically symmetric description of the electron density of hydrogen. Some efforts to provide alternative spherical scattering factors for hydrogen can be found in the literature, but they have never been thoroughly tested by the crystallographic community (e.g., [9]). Unfortunately, and perhaps contrary to expectation, the situation does not improve by refining the hydrogen positions in a conventional multipole model. A number of approaches to obtain approximate hydrogen positions for the use in charge-density studies have been proposed, and will be discussed in Sect. 4.2.

2.2 *Hydrogen Atom ADPs*

There is no doubt that H atoms in molecular crystals vibrate anisotropically; the amplitudes of bond-bending motion are much larger than the amplitudes of bond-stretching motion. Translational and librational molecular motion can also enhance the anisotropy. To use isotropic displacement parameters is a severe approximation, because the isotropic displacement parameters correlate with the monopole parameters of the multipole model, and the quadrupole parameters will include dynamic effects because the quadrupole deformations and the ADPs have the same symmetry. An investigation of the consequences of applying isotropic displacement parameters was given by Madsen et al. [10]; a number of molecular test systems – xylitol [11], urea [12], methylammonium hydrogen succinate monohydrate [13], and methylammonium hydrogen maleate [14]) for which highly accurate X-ray and neutron-diffraction data were available were investigated, and models including isotropic hydrogen displacement parameters were compared to reference models including ADPs derived from the neutron-diffraction experiments. A topological analysis of the static charge density models showed large differences in the electron density and curvature of intramolecular bond-critical points, not only for bonds involving hydrogen atoms. Figure 1 shows the results obtained for xylitol [11]. The bond-critical points mark the boundary between the atomic basins, defined by their zero-flux surfaces within the quantum theory of atoms in molecules (QTAIM) of Bader and coworkers [16]. The volumes and charges of the atomic basins are therefore also affected by the erroneous treatment of hydrogen atoms, which is

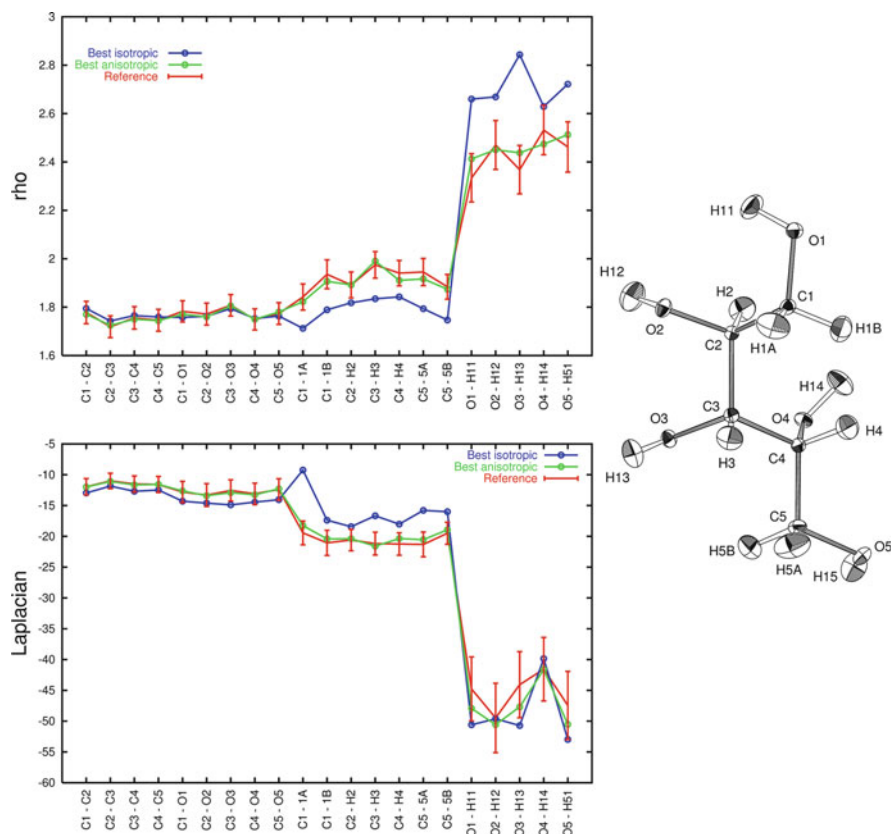


Fig. 1 Electron density [$\text{e} \text{ \AA}^{-3}$] and Laplacian [$\text{e} \text{ \AA}^{-5}$] in the intramolecular bond critical points of three xylitol models. In the reference model (red color) the hydrogen ADPs are based on neutron diffraction data. The error bars correspond to three s.u.s of the properties of this reference model. In the isotropic model (blue) the best possible isotropic description of hydrogen ADPs was employed. The green curve shows the bond critical points from the model using estimated H ADPs (SHADE approach). Modified version of Fig. 4 from Madsen et al. [10]

evident in the study by Hoser et al. [17]. Their work also indicates that it is only meaningful to compare topological properties between different systems when the multipole expansion of the hydrogen atoms are contracted at the same level for all systems. Similar conclusions about the modeling of hydrogen atoms were drawn by Roversi and Destro [18] for topologies and derived electrostatic properties of the electron density; when the description of the hydrogen atoms is limited to an isotropic displacement parameter combined with a contraction of the multipole expansion before the quadrupole functions, the modeling of hydrogen atoms becomes inadequate: A map of the Laplacian of the electron density of the fungal metabolite citrinin [19] shown in Fig. 2a is evidently affected by the isotropic displacement parameters and lack of quadrupole components, as compared to the more elaborate model in Fig. 2b. In the latter case, there is a clear concentration of charge (i.e., an increase in the negative region of $r2q$) toward the acceptor O atoms.

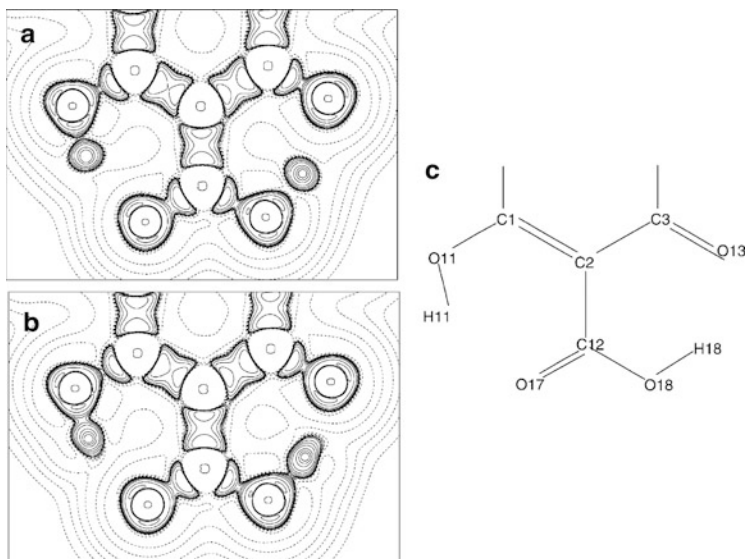


Fig. 2 Laplacian map ($-\nabla^2\rho$) for a fragment of the citrinin molecule [19], adapted from [18]. (a) After refinement of a model with U^{iso} and no quadrupole functions for the H atoms; (b) after refinement of a model with the U^{ij} and quadrupole functions added to the H atoms; (c) atomic numbering scheme

Roversi and Destro further demonstrate that the use of ADPs on H atoms yields electric field gradients (EFGs) at the H nuclei of L-alanine in quantitative agreement with nuclear quadrupole resonance results. Similar agreement with NQR measurements were obtained by Buergi et al. [20] in a study of benzene, as further described in Sect. 5.

The work of Mata et al. [21] examined the influence of including quadrupole functions in the description of the H atom density on the properties of intermolecular interactions. They conclude that these functions in conjunction with hydrogen ADPs have a significant impact on the interaction density, as further discussed in Sect. 5.3

To conclude, there seems to be little doubt that the thermal motion and static charge densities of hydrogen atoms are some of the most difficult to model in charge-density analysis. A proper anisotropic description of the thermal motion combined with a multipole expansion including quadrupole components seems to be the smallest adequate model.

2.3 A Comment on Using the Residual Density and R-Values to Judge the Quality of Models for Hydrogen Atoms

Inspection of residual density plots and R-values are important tools during the construction of a charge-density model. However, these tools cannot stand alone.

The least-squares refinement does not guarantee that the model is physically sound, it merely ensures that we have reached a position in parameter space where the residual is minimized (locally). In the comparison of models with and without estimated ADPs for hydrogen atoms performed by Madsen et al. [10] and Roversi and Destro [18], the change in R-values between the different models was negligible. The less advanced models, using only an isotropic displacement parameter, and in some cases only one bond-directed dipole component and no quadrupole components in the hydrogen multipole expansion are flexible enough to minimize the residual. However, because the model is not physically acceptable, important features of the charge density model are left out. An example that may make the point clear is to consider the position of the hydrogen atom in a standard IAM refinement: The position refines to give an X–H bond length which is way shorter than the position obtained using neutron diffraction data. However, constraining the model to a physically reasonable hydrogen position will probably increase the R-value and give features of negative and positive density in the residual density maps close to hydrogen atoms. Obviously, such features should be removed by improving the quality of the electron density model (e.g., using a multipole description), not by refining the position of the hydrogen atom.

3 How to Obtain H Atom Positions and Anisotropic Displacement Parameters

3.1 *Information from Neutron Diffraction*

A complementary neutron diffraction study is undoubtedly the most reliable source of hydrogen nuclear parameters. However neutron sources are sparse, and the low neutron flux requires millimeter-sized crystals, much larger than the ones needed for the X-ray diffraction experiments. A new generation of neutron spallation sources such as SNS at Oak Ridge National Laboratory (USA) and the ESS (Lund, Sweden) undoubtedly remove some of these barriers, i.e., by allowing much smaller samples and shorter collection times.

The different scattering phenomena and experimental conditions for the X-ray and neutron diffraction experiments cause different systematic errors: thermal diffuse scattering (TDS), extinction and absorption effects are different. The X-ray diffraction experiment is also prone to spectral truncation effects [22]. While absorption effects can be handled by a proper correction based on the morphology of the crystal, and extinction can be taken into account as part of the crystallographic model [23, 24], there is presently few options to deal with the TDS but to cool the crystals to very low temperatures, preferably using helium, to reach temperatures below 20 K [25] thereby diminishing the TDS.

The systematic differences between ADPs from X-ray and neutron diffraction experiments are discussed in detail in the literature [26, 27], and Blessing [26]

provides a practical scaling procedure to account for systematic differences between the non-hydrogen ADPs derived from neutron and X-ray diffraction experiments, in order to use the coordinates and ADPs from the neutron-diffraction experiments as fixed parameters in the refinement of a charge-density model against the X-ray diffraction structure factors.

In some cases neutron diffraction data have a quality and a resolution that merits the refinement of a model including anharmonic motion. The most commonly used model is inclusion of Gram-Charlier coefficients [4, 28]. However, as noted by Kuhs [29], the refinement of these third-order cumulants requires a very extensive dataset, especially at elevated temperatures, where anharmonic motion can be considerable.

Whereas there might be systematic errors affecting the reliability of the ADPs obtained from neutron diffraction, this is much less so for the positions, which are often transferred without any corrections from the model refined against neutron data, to be used as fixed parameters in the refinement against X-ray data. In the absence of results from a neutron diffraction experiment, a number of approaches have been proposed, as discussed below.

3.2 *Estimated Hydrogen Positions*

3.2.1 High-Order Refinement

It is well known that the accuracy of the atomic positions of non-hydrogen atoms obtained from X-ray diffraction experiments can be improved by refining an IAM against the high-order reflections (i.e., $\sin(\theta)/\lambda > 0.7 \text{ \AA}^{-1}$, see the work by Ruysink and Vos [30]). The reason is that the relative contribution of the core electrons to the reflection intensities increases with resolution, and in this way the shifts in atomic positions due to the modeling of bonding density [31] can be diminished. However, hydrogen atoms have no core electrons, and the advantages of this approach seem less obvious for the determination of hydrogen atomic positions. Hope and Ottersen [32] tested this approach in a study of s-diformohydrazide and found considerable improvements in the bond-lengths involving hydrogen atoms. Almlöf and Ottersen [33] have given a theoretical analysis of the high-order refinement of hydrogen positions. Some improvement was also seen by Madsen et al. [10] for xylitol, however in that case other methods proved to be in closer agreement with neutron diffraction results, as described below.

3.2.2 A Polarized Hydrogen Atom

Realizing that the refinement of a spherical scattering factor against X-ray structure factors is not sufficient to provide hydrogen positions in agreement with neutron

diffraction results Stewart and coworkers [34] proposed that the use of a fixed multipole expansion for a bonded hydrogen atom could be used to obtain a more accurate determination of the time proton positions in molecular crystals.

This idea has been implemented in the VALRAY program [35] and used for X-ray charge-density analysis. This *polarized hydrogen atom* consists of spherical component (single-exponential type) and a bond-directed dipole. The population of the dipole and the spherical components is kept fixed during the refinement, and only the position and isotropic displacement parameter of the hydrogen atom is refined.

Destro and coworkers have used this approach in a range of studies (e.g., [19, 36–38]) and were able to obtain X–H bond-lengths close to the typical values found in neutron-diffraction studies, although no direct comparison with neutron diffraction measurements was made.

Madsen et al. [10] tested the polarized hydrogen atom in refinements against X-ray structure factors of xylitol and compared the results to the positions obtained from neutron diffraction [11]: The polarized hydrogen atom was an improvement compared to the SDS scattering factor, but not as efficient as the posteriori elongation of X–H bond lengths to match mean values from neutron diffraction experiments.

3.2.3 Neutron Mean Values

While the high-order refinements and polarized hydrogen atom model are attempts to obtain the hydrogen positions based on the X-ray diffraction data, a more pragmatic procedure is to base the positions on statistical material from a large pool of structures determined from neutron diffraction data.

The International Tables for Crystallography [39] contains a wealth of information on X–H bond lengths based on data from the CSD database. Once the direction of the X–H bond has been established by refinement against the X-ray data, the bond can be extended to match the mean values derived from neutron diffraction experiments. This procedure has been used in numerous charge-density studies (some very recent examples are Overgaard et al. [40]) and seems to give the best possible estimate of the hydrogen positions. Madsen et al. [10] found for xylitol that the mean deviation from the neutron result was 0.012(8) Å in bond lengths, corresponding to a mean deviation in positions of 0.041(19) Å.

The X–H bond-lengths depend on the number and strength of the hydrogen bonds that the X–H group is involved in [41], and this information could in principle be used to improve the estimates of hydrogen positions.

3.2.4 A Combined Approach

Hoser et al. [17] analyzed models for a series of 1,8-bis-(dimethylamino)naphthalene (DMAN) salts of organic counter-ions. They conclude that a combined

approach involving high-order refinement of the non-hydrogen atoms combined with low-order refinement of the hydrogen atoms and subsequent elongation of the X–H bond lengths to match mean-values derived from neutron diffraction studies gives the best results as compared to complementary neutron-diffraction studies.

3.3 *Ab Initio/Hirshfeld Atom Refinement*

A sophisticated extension of the improved aspherical scattering factors for hydrogen atoms used in the polarized H atom model is the refinement strategy of Jayatilaka and Dittrich [42], which is a least-squares refinement against X-ray diffraction data of transferable atomic densities defined in terms of “Hirshfeld atoms.” The atoms are defined by using Hirshfeld’s stockholder partitioning [43] of an electron density obtained from quantum mechanical calculations. The strategy was tested by refining against X-ray data for urea and benzene, and benchmarked against neutron diffraction results. The C–H and N–H bond distances are remarkably within 0.01 Å of the neutron diffraction results. The approach yields ADPs of the carbon and hydrogen atoms of benzene in excellent agreement with the neutron diffraction data. However, for urea the results are a bit ambiguous with some ADPs in excellent agreement with neutron diffraction results, others deviating more than 50%, and a large dependence on whether the applied electron density was obtained using Hartree–Fock (HF) or density functional theory (DFT) methods. This approach seems very promising, but it has to be further validated on more structures before any conclusions can be drawn as to its general applicability to obtain positions and ADPs for hydrogen atoms.

3.4 *Estimated H ADPS Based on a Combination of Rigid Body Motion and Internal Motion*

The method of estimating hydrogen ADPs based on a combination of rigid body motion derived from the ADPs of the non-hydrogen atoms and internal modes taken from other experiments was pioneered by Hirshfeld and coworkers [44–47]. It is based on the idea that it is possible to consider the atomic motion in molecular crystals as a combination of external rigid-body motion and internal motion corresponding to high-frequency molecular vibrations, such as bond-bending and bond-stretching modes. The analysis is based on the assumption that the rigid-body and internal motions are uncorrelated, and that the components of B , the atomic mean square displacement matrix – and thereby the U matrix of ADPs – can be obtained as a sum of the two contributions

$$U^{ij} = U_{\text{rigid}}^{ij} + U_{\text{internal}}^{ij}. \quad (6)$$

The external motion is taken from a rigid-body or segmented rigid-body analysis of the non-hydrogen ADPs, while the internal motion can be estimated from spectroscopic experiments, analysis of neutron diffraction data, or based on *ab initio* calculations. These three different approaches are discussed below – a thorough comparison has been given previously [2].

3.4.1 The Rigid Body Motion

Because the intermolecular forces are weak compared to intramolecular forces, the external molecular vibrations have larger amplitudes and lower frequencies than the internal modes. The atomic motion of the non-hydrogen atoms is therefore mostly due to the external molecular vibrations. A commonly used model is to regard the molecules in the crystal as vibrating as rigid bodies, independently of the surrounding molecules, and experiencing the mean potential of these molecules. This rigid-body model, used to analyze the ADPs of the non-hydrogen atoms, was introduced by Cruickshank [48] and refined by Schomaker and Trueblood [49] into what is known as the TLS model and has been used in numerous studies [50]. An excellent introduction to the TLS analysis is given by Dunitz [51].

The rigid body assumption can be relaxed in different ways to include torsional vibrations or other large-amplitude vibrations [52]. The TLS model is implemented in the THMA program of Schomaker and Trueblood, as well as in the Platon program [53]. A related normal-mode analysis is provided by the program EKRT by Craven and coworkers [54, 55], and by the program NKA of Buergi and coworkers [56]. The latter program is furthermore able to refine a model against ADPs from multi-temperature experiments [57, 58].

The quality of the rigid body model is normally judged by computing a residual defined as

$$R_w(U^{ij}) = \sum_{i,j} w_{ij} \frac{U_{\text{measured}}^{ij} - U_{\text{TLS model}}^{ij}}{U_{\text{measured}}^{ij}}, \quad (7)$$

where w_{ij} is the weight used in the least squares fit of the TLS model against the observed ADPs U_{measured}^{ij} . The TLS analysis of well-determined ADPs of truly rigid bodies (e.g., benzene) often gives $R_w(U^{ij})$ values of about 5%, especially for low-temperature studies. For less rigid systems values of 8–12% are common. For the purpose of estimating hydrogen ADPs, the TLS models of these less rigid systems still seem to give good results. Apart from this residual, an excellent way to judge the rigidity of a system is to compare the differences $\Delta_{AB}(\langle u^2 \rangle)$ in mean square displacements along all atom–atom vectors in the molecule [59]. In a truly rigid body these differences should be exactly zero. However, even in rigid molecules, atoms of different mass will have small differences in internal mean square displacements due to the internal vibrations, giving rise to $\Delta_{AB}(\langle u^2 \rangle)$ values on the order of 10^{-4} \AA^2 .

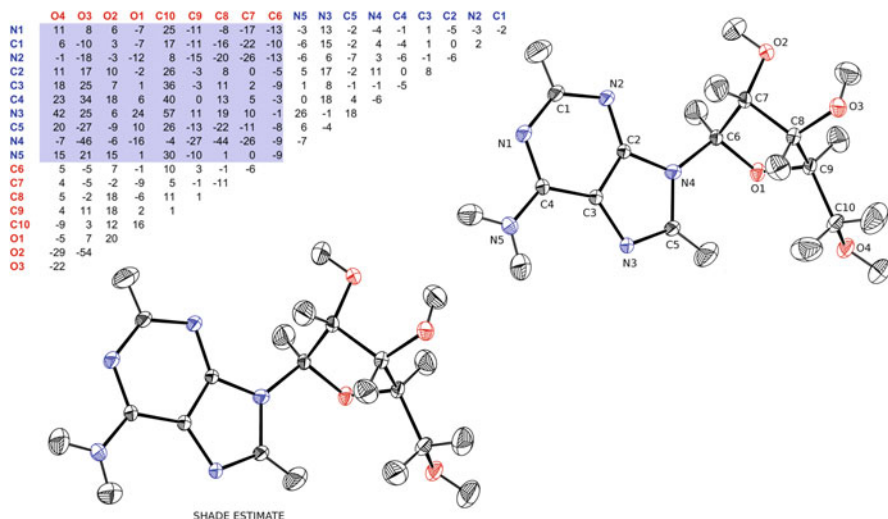


Fig. 3 Matrix of differences in mean square displacements [10^{-4} \AA^2] along interatomic vectors for the non-hydrogen atoms of adenosine [60]. The shaded region corresponds to the differences between the atoms of the two “rigid” segments of adenosine. The plots of equal-probability ellipsoids for adenosine (50% probability level) correspond to the ADPs estimated using SHADE (*left*) and the values obtained from neutron diffraction experiments, respectively (*right*)

A matrix of such differences for adenosine is given along with plots of equal-probability ellipsoids of measured and estimated ADPs in Fig. 3. The differences are very small between bound atoms in accordance with the “rigid bond test” of Hirshfeld [45], but quite large between the atoms in the adenine and ribose moieties. Accordingly, Klooster and coworkers [60] found that a segmented rigid body model that allows torsional motion about the glycosidic bond N4–C6 was the most satisfactory model. It gives a drop in $R_w(U^{ij})$ from 13.4% to 8.7%. This model was used to test the segmented rigid body approach for estimating hydrogen ADPs [2] as discussed in Sect. 4.4.4.

Once the rigid-body motion of the molecule has been assessed by analysis of the non-hydrogen ADPs it is straight forward to calculate the U_{rigid}^{ij} of the hydrogen atoms based on the rigid body motion. The formulas to perform this calculation can be found in the original literature on the different rigid body analysis approaches.

3.4.2 The Internal Motion

It is well known from Raman and infrared spectroscopic studies that the internal vibrations of hydrogen atoms depend on the chemical environment. First of all, the bond-stretch vibration depends on the type of atom hydrogen is bound to. For example, the stretch-frequency of an O–H bond is much larger than the corresponding frequency of a C–H bond. Second, the functional group influences

the bond-bending frequencies, e.g., the out-of-plane vibration of an ethyl group has a larger amplitude than the corresponding vibrations of a methine group. The methods described in the following all assume that these internal vibrations are uncorrelated from the intermolecular or external modes.

The general theoretical framework used to calculate the internal contribution to the ADPs is basically the same whether these estimates are based on information from ab initio calculations, spectroscopic evidence, or neutron diffraction experiments on related compounds. The vibrational modes are expressed in terms of normal coordinates and normal mode frequencies. The modes are uncoupled; each is considered to be an independent harmonic oscillator.

The general relation between vibrational normal mode coordinates and the atomic mean square displacement matrix $\mathbf{B}(k)$ is [3]:

$$\mathbf{B}(\kappa) = \frac{1}{Nm_\kappa} \sum_{j\mathbf{q}} \frac{E_j(\mathbf{q})}{\omega_j^2(\mathbf{q})} \mathbf{e}(\kappa|j\mathbf{q}) \mathbf{e} \times (\kappa|j\mathbf{q})^T, \quad (8)$$

where $e(k|jq)$ represents the k th component of a normalized complex eigenvector $e(jq)$, and corresponds to atom k in normal mode j along the wavevector q . ω_j is the frequency of mode j and $E_j(q)$ is the energy of the mode, given by

$$E_j(\mathbf{q}) = \hbar\omega_j(\mathbf{q}) \left(\frac{1}{2} + \frac{1}{\exp(\hbar\omega_j(\mathbf{q})/k_B T) - 1} \right). \quad (9)$$

In these equations, the energy and frequency of the normal modes depend on the wavevector q . For high-frequency internal molecular vibrations this dependence is negligible, and the equations above can be approximated by

$$\mathbf{B}(\kappa) = \frac{1}{Nm_\kappa} \sum_j \frac{E_j}{\omega_j^2} \mathbf{e}(\kappa|j) \mathbf{e} \times ((\kappa|j))^T \quad (10)$$

and

$$E_j = \hbar\omega_j \left(\frac{1}{2} + \frac{1}{\exp(\hbar\omega_j/k_B T) - 1} \right). \quad (11)$$

Where $\mathbf{B}(k)$ is the atomic mean square displacement matrix of atom k . The mean square displacement matrix \mathbf{B} is expressed in a Cartesian coordinate system and is related to the matrix \mathbf{U} of ADPs by a similarity transformation, since the ADP matrix is expressed in the generally oblique coordinate system defined by the unit cell axes. The definitions and transformation properties of ADPs can be found in, e.g., the report by Trueblood et al. [4] or the International Tables for Crystallography [28].

The methods differ in the way that the vibrational coordinates and frequencies are obtained and described, and in the number of modes that is used to construct the internal mean square displacement matrix of the hydrogen atoms.

3.4.3 Spectroscopic Evidence

In his early papers, Hirshfeld used information from Raman and infrared spectroscopy to assess the frequencies and corresponding mean square displacements of the bond-stretching and bond-bending modes of the X–H bonds [46, 47]. This approach has been used several times by Destro and coworkers [37, 38, 61–63]. The procedure has been implemented in the code ADPH and has been described and tested in detail by Roversi and Destro [18];

ADPH: In the ADPH approach the normal mode frequencies are based on spectroscopic data and each vibration is described by approximate vibrational coordinates. In the simplest case, three independent modes – one bond-stretching mode and two modes perpendicular to the bond – are used to construct the internal part U_{internal}^{ij} of the internal mean square displacement matrix for the hydrogen atom, however there is no limitation on the number of modes that can be used. This approach has the advantage that the estimates of internal ADPs can be based on experimental evidence on the same compound that is studied by X-ray diffraction. However, for larger molecules with several similar functional groups, it becomes difficult to assign the different spectroscopic frequencies to the right hydrogen atoms, and the approach has to rely on mean group frequencies.

3.4.4 Analysis of Neutron Diffraction Data

It is possible to analyze the vibrational motion of hydrogen atoms in a similar vein as the statistical analysis of X–H bond lengths derived from neutron diffraction studies found in International Tables for Crystallography [39]. When the total atomic mean square displacement matrix U^{ij} has been determined from neutron diffraction experiments, and the rigid molecular motion U_{rigid}^{ij} has been determined from a rigid-body analysis of the non-hydrogen ADPs, it becomes possible to get an estimate of the internal motion of the hydrogen atoms by rearranging (6).

$$U_{\text{internal}}^{ij} = U^{ij} - U_{\text{rigid}}^{ij}. \quad (12)$$

It was noted by Johnson [64] that the mean square displacements derived from U_{internal}^{ij} of hydrogen atoms was in good agreement with spectroscopic information, showing systematic trends corresponding to the functional group that hydrogen was part of. Similar observations were done by Craven and coworkers in the analysis of cholesteryl acetate [65], suberic acid [66], hexamethylene tetramine [67], and piperazinium hexamoate [68]. The internal torsional motion of a range of librating

groups, including methyl, carboxyl, and amino groups was also thoroughly investigated by Trueblood and Dunitz [69] based on more than 125 neutron diffraction studies of molecular crystals from the literature.

Madsen and coworkers [11] investigated the internal mean square displacements of hydrogen atoms in xylitol and a range of related carbohydrate compounds found in the literature, and these estimates of internal modes of were collected in a “library” and later improved and enhanced with more statistical material [2]. The present library provides mean values of internal stretch modes as well as in-plane and out-of-plane bending modes for a range of chemical groups involving hydrogen bound to C, N, and O, and forms the basis for assigning ADPs to hydrogen atoms in the *Simple Hydrogen Anisotropic Displacement Estimator* (SHADE) server.

SHADE: The library of internal mean square displacements derived from neutron diffraction studies has been used to construct a web server that allows fast and accurate estimates of the ADPs of hydrogen atoms. The SHADE server [70] allows users to submit a CIF file [71] containing the atomic coordinates and the ADPs of the non-hydrogen atoms. The server performs a TLS analysis using the THMA11 program, and combines the rigid body motion with the internal motion obtained from analysis of neutron diffraction data. It is possible to perform a segmented rigid body analysis using the attached rigid group approach of the THMA11 program [2, 52]. The segmented rigid body approach seems to give marginally better results, as compared to neutron diffraction experiments, as judged from a few test cases [2] on non-rigid molecules. For adenosine we observed that despite the improved description of the motion of the heavy-atom skeleton, only small improvements were observed for the H atom ADPs. For some hydrogen atoms there was a substantial improvement, while for other we observed a worsening agreement. There is definitely room for further testing and improvement of the segmented rigid body analysis in this context.

The SHADE server is available at the web address: <http://shade.ki.ku.dk>.

3.4.5 Ab Initio Calculations

Estimates of interatomic force-constants obtained from ab initio calculations are today a straightforward way to build the dynamical matrix used in a normal-mode coordinate analysis. Several academic and commercial ab initio codes offer integrated normal-mode analysis. A program XDvib which is part of the charge-density analysis program XD [72] is able to read the output from a normal-mode analysis from Gaussian [73] and compute the ADPs corresponding to internal vibrations. This procedure was used successfully by Flaig et al. [74] to provide ADPs for hydrogen atoms in a study of D,L-aspartic acid. In that study, the external contribution to the ADPs was based on a rigid-link refinement of the non-hydrogen ADPs, which essentially mimics a rigid-body type refinement. However, the ab initio calculation of internal modes was performed on an isolated (gas-phase) molecule. This is not always sufficient to obtain reliable results. Results by Luo et al. [68] and Madsen et al. [11] show that gas-phase calculations can lead to

internal mean square displacements that are much larger than the total mean square displacements as derived from neutron diffraction experiments, because the intermolecular potential energy surface (PES) of an isolated molecule is very different from the PES of a molecule in a crystalline environment, especially for non-rigid systems with large amplitude torsional vibrations. The flat PES causes large amplitudes of some of the internal molecular vibrations, e.g., torsional modes. In these cases, it is necessary to take the intermolecular environment into account. For rigid molecules with weak intermolecular interactions it may be sufficient to use gas-phase calculations (e.g., the case of naphthalene [75]). One of the major advantages of the *ab initio* approach is the possibility of estimating the motion of hydrogen atoms that are in nonstandard environments, i.e., hydrogen atoms in groups that are not well characterized by spectroscopy or neutron diffraction measurements.

TLS+ONIOM: Whitten and Spackman [76] used ONIOM calculations – a procedure where the central molecule is treated using quantum mechanics and a cluster of surrounding molecules is treated using classical molecular mechanics – to mimic the intermolecular environment with excellent results. This “TLS+ONIOM” approach differs slightly from the ADPH and SHADE approaches in that the internal mean square displacements are subtracted from the ADPs of the non-hydrogen atoms before the TLS analysis. Although this is a small correction, it seems to be an improvement as it diminishes the differences between the mean square displacements of bonded atoms in the direction of the bond (this so-called rigid bond test by Hirshfeld [45] is often used to test the reliability of ADPs derived from experiments). An alternative approach is to use a program that is designed for *ab initio* periodic solid-state calculations. An approach based on the CRYSTAL09 program has been tested by Madsen et al. [77] and gives results in close agreement with the TLS+ONIOM calculations.

3.5 *Estimates of H ADPs Based Solely on Force-Field or Ab Initio Calculations*

The internal vibrations of hydrogen atoms correspond to the high-frequency part (200–3,500 cm^{-1}) of the Raman and IR spectra. It is well known that these frequencies can be reproduced by *ab initio* calculations, at least to within a common scale factor (see Scott and Radom [78]) – as witnessed by the success of the TLS+ONIOM approach described above.

However, the low-frequency (0–200 cm^{-1}) external vibrations of hydrogen and non-hydrogen atoms give a significant contribution to the mean square displacement matrix, and this contribution is increasing with temperature, according to (10) and (11). The low-frequency vibrations are more complicated to compute because they correspond to correlated molecular motion and show dispersion, i.e., the frequencies depend on the direction and magnitude of the wavevector. It is possible

to estimate these normal modes by using a lattice-dynamical approach, as developed by Born and von Kármán and described in the classical book by Born and Huang [79], and in a language more familiar to crystallographers by Willis and Pryor [3].

The lattice-dynamical evaluation of ADPs based on the Born and von Kármán procedure has been applied for many years based on empirical force-fields. A series of systematic calculations on several rigid molecular crystals, and comparison with experimental results was reported during the 1970s by Fillippini, Gramaccioli, Simonetta, and Suffriti [80–82]. Later results by Criado and coworkers showed that the force-field approach was also sufficient for azahydrocarbons [83]. In these studies it is sometimes found that the calculated ADPs are higher – in some cases by more than 50% – than the experimental results. Gramaccioli and coworkers ascribe this difference to the effect of TDS on experimental ADPs [81, 82], which, because it is seldom corrected for, leads to an increase in the observed diffraction intensities and thereby small ADPs. However, in cases where the force-constants of the Born and von Kármán model are derived from inelastic neutron scattering measurements and infrared spectroscopic measurements, as in the study of urotropine by Willis and Howard [84] and the study of silicon by Flensburg and Stewart [85], there seem to be an excellent agreement with the experimental ADPs, so perhaps some of the discrepancies are due to inadequacies in the applied empirical force fields.

With today's computer power, it has become feasible to perform *ab initio* calculations in order to assess the force-constants needed for the lattice dynamical treatment. Whereas the *ab initio* approach seems to work very well for extended solids [86, 87], very little work has been done to test it for molecular crystals. Work in progress [77] on estimation of ADPs for crystalline urea, urotropine, and benzene indicates that the well-known inability of DFT methods to account for dispersive forces may be a major problem for computing the lattice dynamics, and thereby the ADPs, of molecular crystals using DFT methods.

4 Charge-Density Studies with a Special Focus on H Atoms

All charge-density studies of molecular crystals involving hydrogen atoms are to some extent affected by the modeling of the hydrogen atoms. However, some studies focus specifically on the intermolecular interactions, often in terms of hydrogen bonding, or on the properties of the hydrogen atoms, e.g., their electronic properties in terms of the EFGs. In these cases the treatment of hydrogen is of course crucial. Here, we discuss a number of cases where the role of hydrogen atoms have proven to be especially important – and where the authors have considered the modeling of hydrogen carefully – in order to discuss the pros and cons of the different approaches to hydrogen modeling. The list of studies is not meant to present an overview of recent charge-density studies involving hydrogen atoms, but rather a few highlights that will give an impression of limitations and possibilities of different approaches to model and study hydrogen atoms.

4.1 Strong Hydrogen Bonds

Very short and strong hydrogen bonds possess many unique characteristics [1], and they often play an important role in biological systems [88]. Charge-density studies have been used to characterize the electronic environment in the vicinity of the proton involved in strong O–H...O bonds. Is the hydrogen bond symmetric? Does the proton have a unimodal or bimodal probability density distribution – i.e., is it situated in a single or double-well potential? Do the very strong hydrogen bonds resemble the weaker hydrogen bonds or should they rather be characterized as covalent?

MAHS and MADMA: In order to answer these subtle questions, it is important to gather as much information about the hydrogen nuclear parameters as possible. Flensburg and coworkers [13] studied the salt of MAHS – methylammonium hydrogen succinate monohydrate – based on the combined use of neutron and X-ray diffraction data at 110 K. Based on the neutron diffraction data they found that the short O–H...O hydrogen bond was symmetric. A topological analysis of the model of static electron density showed that the hydrogen bond had covalent character; the hydrogen atom formed covalent bonds to both oxygen atoms. These conclusions were confirmed in a subsequent study of MADMA – methylammonium dihydrogen maleate [14].

Benzoylacetone: Madsen and coworkers [89] carried out a study of the intramolecular hydrogen bonding in benzoylacetone (1-phenyl-1,3-butadiene) using 8.4 K X-ray data and 20 K neutron data. In contrast to the symmetrical arrangement of the hydrogen atom found in MAHS and MADMA, the hydrogen atom engaged in the strong hydrogen bond in benzoylacetone is asymmetrically placed in a large flat potential well. A topological analysis of the keto-enol group containing the strong intramolecular hydrogen bond showed that the hydrogen position was stabilized by both electrostatic and covalent bonding contributions at each side of the hydrogen atom.

Isonicotinamide: A recent study of two polymorphs of isonicotinamide and oxalic acid investigated the character of short strong O–H...N intermolecular hydrogen bonds between the acid and the pyridine base [90]. Again, combined X-ray and neutron diffraction techniques were crucial to deconvolute a static electron density from the mean thermal charge density. As for the O–H...O bonds, it was found that the hydrogen bonding had a pronounced covalent character. This study was compared to the charge density obtained from periodic ab initio calculations on the crystalline system.

In these studies where the fundamental questions are related to the exact position and dynamics of the protons, the use of spectroscopic information, or information from ab initio calculations, can provide useful complementary information about the dynamics of the proton, however they cannot provide the detailed information about the mean position of the proton which is crucial for the deconvolution of the dynamics of the static density from the vibrations.

There seems to be no way around using a neutron diffraction approach, in order to get a deconvoluted picture of the motion of the nuclei and the distribution of the electron density. However, if the researcher is prepared to abandon the idea of deconvolution, maximum entropy methods can provide an experimental *vibrationally averaged* electron density, which may answer some of the questions posed previously – does the proton occupy a single or double potential well? How is the strength and covalency of the bonds? Studying the electrostatic potential in the region around the hydrogen bond in question, using a multipole model approach where the hydrogen atom remains unmodeled, may provide some of the same information, as shown in the study by Flensburg and coworkers [13].

In other studies of hydrogen-containing molecules, the focus is a characterization of the intermolecular bonding, not the exact position of a hydrogen atom. In these cases, the estimated hydrogen positions and anisotropic thermal motion might be sufficient, as discussed later (Sect. 5.3).

4.2 EFGs at the H Nuclei

A study that certainly merits attention for its careful treatment of hydrogen atom motion is the charge-density study of benzene carried out by Bürgi et al. [20]. This study demonstrates that neutron diffraction data can be useful even if the data have been collected at other temperatures than the X-ray diffraction experiment. Bürgi and coworkers analyzed neutron diffraction data on benzene collected at 15 and 123 K in terms of a normal-coordinate analysis of ADPs [57, 58]. In this analysis, the temperature-dependent rigid-body motion is separated from the high-frequency internal motion which is temperature independent. In essence, it is a multi-temperature TLS analysis also including parameters to account for the internal motion. The resulting normal coordinate model was then used to derive ADPs for the hydrogen atoms at the desired temperature, which in this case was 110 K. The hydrogen ADPs were then used as fixed parameters in a very elaborate multipole model refined against the X-ray diffraction data. The multipole expansion extended up to the hexadecapole level for the carbon atoms, and up to the quadrupole level for hydrogens as noted by the authors, the latter is essential for a proper description of the deformations of quadrupole symmetry about the H atoms, and crucial in this case; from the model of the static electron density, Bürgi and coworkers were able to derive EFGs at the hydrogen nuclei in quantitative agreement with measurements of nuclear quadrupole coupling constants derived from nuclear quadrupole resonance spectroscopy. This is an important confirmation that the hydrogen nuclear parameters are of an excellent quality. As noted by Brown and Spackman [91], EFGs are sensitive to charge density features involving core electrons which, to be accurately modeled, would require more extensive high-angle diffraction data than are currently available, and a more flexible multipole model. For hydrogen atoms, which lack core electrons, the situation is less prohibitive, but still requires a very elaborate multipole model. As a further confirmation of the quality of the model, the

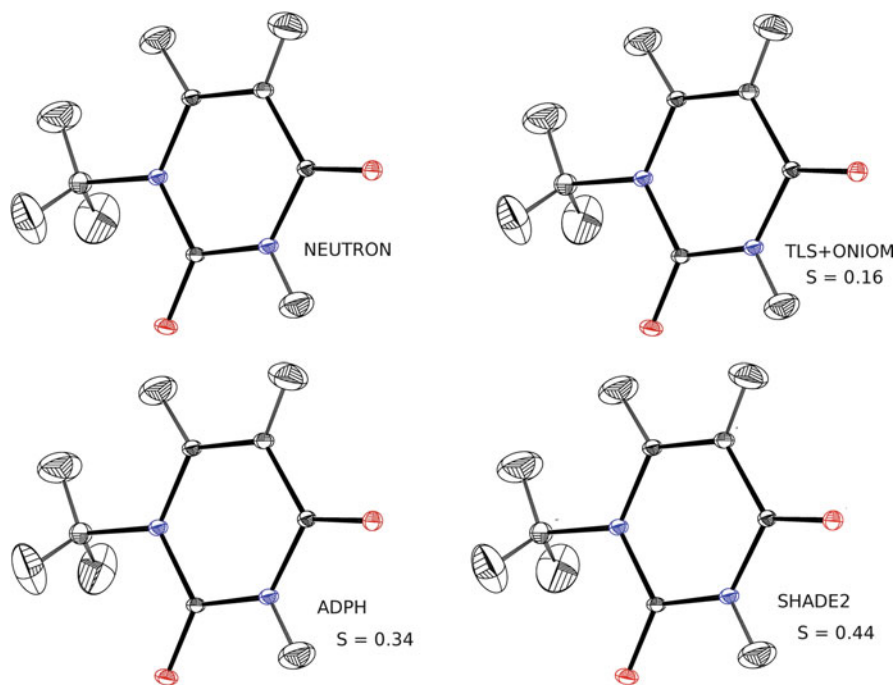


Fig. 4 A comparison of methods to estimate the hydrogen ADPs of 1-Methyl Uracil, based on the work by Munshi and coworkers [2]. To the right of each ellipsoid plot, we give the similarity index [15] between the neutron-derived and estimated ADPs. Equal-probability ellipsoids are shown at the 70% probability level

molecular quadrupole moment derived from the total charge density of the molecule in the crystal also shows to be in excellent agreement with measurements made in the gas phase and in solution. Bürgi and coworkers used neutron diffraction experiments to obtain the hydrogen nuclear parameters. But coordinates and ADPs based on the ADPH approach (Sect. 4.4.3), in conjunction with an elaborate multipole model, seem adequate in order to obtain EFGs at the hydrogen nuclear positions, as judged from the study by Destro et al. on α -glycine [37]. This opens the possibility that also the TLS+ONIOM and SHADE approaches are sufficiently accurate for this type of study (Fig. 4).

4.3 Molecular Interactions

One of the areas where estimated hydrogen ADPs and positions may play an important role is in the study of biologically important molecules, where experimental charge densities are used in the characterization of the electrostatic properties of the molecules and their intermolecular interactions.

Fidarestat: A very recent example is the study of Fidarestat, an inhibitor of the protein human aldose reductase [92]. In this study the hydrogen atoms were restrained to the standard neutron distances as listed in the International Tables for Crystallography [39], and a preliminary multipole refinement was conducted using isotropic displacement parameters and an SDS scattering factor [5] for the hydrogen atoms. Subsequently, the positions and ADPs from this refinement were submitted to the SHADE server [70] in order to estimate ADPs for the hydrogen atoms. The molecule was divided into four rigid groups in the TLS analysis. The hydrogen atom ADPs were then refined using tight restraints to the target values obtained from the SHADE program, and the multipole refinement was then continued. The authors noticed a small, but systematic improvement in the agreement factors on adoption of the anisotropic hydrogen atom description. After inclusion of ADPs for hydrogen the authors did not observe significant unmodeled electron density around the hydrogen atoms, and chose to contract the multipole expansion at the dipole level for the hydrogen atoms. An analysis of the electrostatic potential mapped on the molecular surface (Fig. 5) showed clearly visible

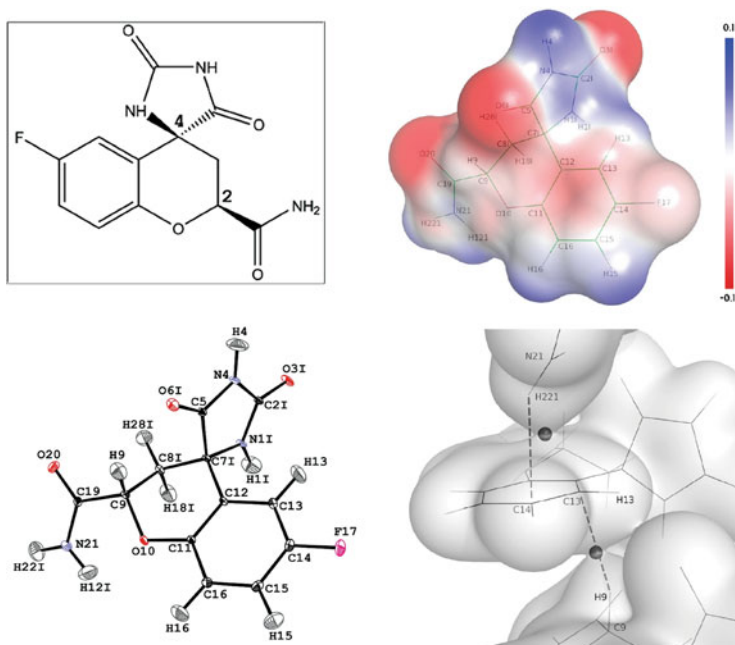


Fig. 5 OrtepIII representation [93] of fidarestat with thermal displacement ellipsoids plotted at 50% probability and the chemical diagram of fidarestat in a frame. Deformation electrostatic potential $\Delta\phi$ (e/Å) generated by the isolated fidarestat molecule mapped on the solvent-excluded surface with a probe radius of 1.4 Å. The potential $\Delta\phi$ was derived from the deformation electron density $\Delta\rho$. The view was made with the program Pymol [94]. View of the hydrogen bonds with π acceptors in a trimer of fidarestat molecules. The aromatic ring containing the C13–C14 atoms is involved on both sides in H... π -system bonds represented as *gray dashed lines*. The electron density cutoff value for the iso-surface is +0.05 e/Å³. The view was made with the program Pymol [94]

polar binding sites, related to the stronger positive charges of the H–N hydrogen atoms bound to nitrogen atoms compared to H–C atoms. The electrostatic potential pattern was complementary, in a key–lock manner, with the charges of the hydrogen bonded groups in the human aldose reductase active site. A topological analysis of the hydrogen bonding pattern revealed notable $\pi\cdots H-X$ hydrogen bonds of a strength comparable to C–H \cdots O hydrogen bonds, giving significant contributions to the crystal packing energy.

In this case, the use of estimated hydrogen nuclear parameters seems adequate in order to draw conclusions based on analysis of electrostatic potentials and topological analysis of intermolecular interactions. However, some controversies remain regarding whether it is possible to measure the changes in electron densities due to intermolecular interactions with the present accuracy of experimental charge density studies, as discussed in the following.

Interaction densities: An ongoing debate is whether the quality of present-day experimental charge density studies makes it possible to determine the changes in the charge density due to the interaction with neighboring molecules in the crystal – the interaction density. The charge densities in the intermolecular regions are of a similar magnitude as the typical standard uncertainty of the electron density. A study based on model charge densities obtained from periodic HF calculations on ice VIII, acetylene, formamide, and urea performed by Spackman et al. [95] concluded that the multipole model is capable of qualitative retrieval of the interaction density. The study of Spackman et al. included the effects of thermal motion of the refined electron densities, however no account was taken of the effect of random errors in the simulated structure factors. This effect was included in a subsequent theoretical study of urea by Feil and coworkers [96], which made it impossible to retrieve the interaction density for simulated data.

In a more recent study by Dittrich and Spackman the retrieval of interaction densities was addressed using an experimental charge-density study of the amino acid sarcosine, combined with periodic ab initio calculations using the CRYSTAL98 program [97]. In lack of neutron diffraction data the thermal motion of the hydrogen atoms was based on the TLS+ONIOM approach. Hydrogen positions with bond-lengths in agreement with mean values from neutron diffraction studies were obtained by imposing an electron density model from the invariom database. Dittrich and Spackman conclude that it is possible to retrieve an interaction density from the multipole model of sarcosine, but only if the hydrogen atom electron density was based on the invariom database [98]. The authors note that *it appears that such a highly constrained multipole model is necessary to observe fine details with current data, as the scattering signal of the H atoms is unfortunately rather small when compared to C, N or O atoms.*

Hydrogen bond energies: Closely related to the retrieval of interaction densities is the analysis of intermolecular hydrogen bonding. The standard uncertainty of electron density maps obtained by fitting multipole models against X-ray diffraction data is normally about $0.05\text{ e}/\text{\AA}^3$. The electron density of intermolecular bond-critical points is often only a few times higher than this. How reliable is the information obtained from analysis of the electron density in the intermolecular region?

Espinosa and coworkers [99–101] found that the topological properties decay exponentially with the $d_{H\cdots A}$ distance in an analysis of 83 X–H \cdots O interactions from 15 different experimental electron-density studies performed by different investigators using a large variety of models for the hydrogen atoms. However, in a later study of L-histidinium dihydrogen orthophosphate orthophosphoric acid (LHP) [102], it was found that models of hydrogen atoms including quadrupole functions show a quite different behavior – deviating from the exponential dependence – in contrast to models where the multipole expansion is contracted at the dipole level (Fig. 2). The quadrupoles of the H atoms sharpen the electron-density distribution in the plane orthogonal to the H \cdots A hydrogen-bond direction, increasing the perpendicular curvatures and therefore decreasing the Laplacian magnitude at the BCP. Hydrogen-bond interactions that are found as pure closed shell (HCP > 0) in the refinements undertaken without quadrupolar terms present a significant shared-shell character (HCP < 0) when these terms are included. As a consequence, results coming from the models that describe the H atoms up to dipolar terms appear to be in better agreement with theoretical calculations [103] (Fig. 6).

Analysis of intermolecular interactions in epimeric compounds: In a study of the epimeric compounds xylitol and ribitol by Madsen and Larsen [104], it was only

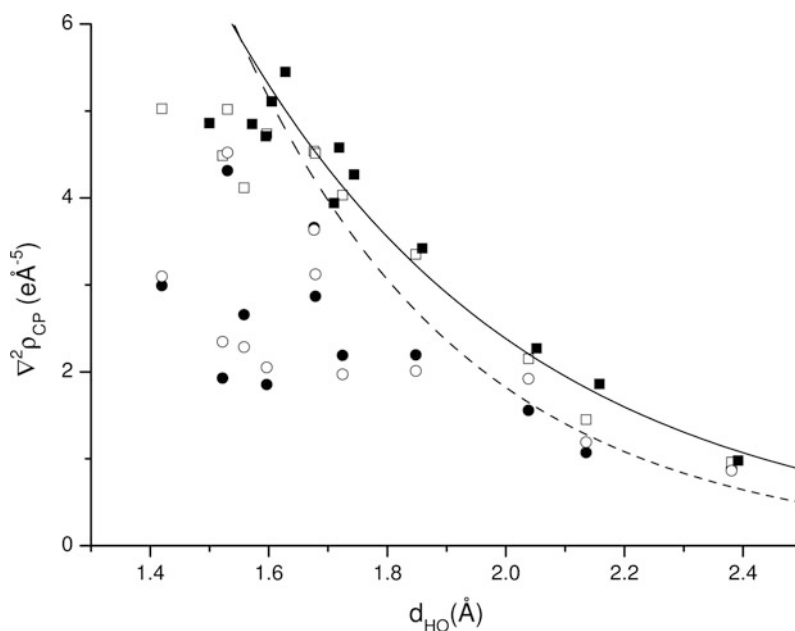


Fig. 6 Topological properties at the BCPs of the hydrogen bonds observed in L-histidinium dihydrogen orthophosphate orthophosphoric acid versus H \cdots O distance. *Open and filled circles* correspond to models including quadrupole functions on the hydrogen atoms, *open and filled squares* correspond to models without quadrupole functions on hydrogen. The curves correspond to the empirical dependences by Espinosa et al. [100]. *Solid lines* for X-ray only and *dashed lines* for X-ray+neutron refinements

possible to obtain neutron diffraction data for xylitol because it was impossible to grow crystals of a sufficient size for ribitol. The hydrogen positions for ribitol were based on an IAM refinement and extended to the standard values based on neutron experiments. Hydrogen ADPs were estimated using the SHADE server. A quite elaborate model of the hydrogen electron densities was used, with the multipole expansion extending to the quadrupole level, and with a radial part having a common k parameter for the hydrogen atoms bound to oxygen, and another for the hydrogen atoms bound to carbon. A topological analysis of the intermolecular interactions indicated that the two compounds had identical interaction energies, in agreement with results obtained from calorimetric measurements and periodic DFT calculations. Differences in melting point and mass density could therefore not be explained as a consequence of differences in solid state enthalpies, but were instead related to a difference in solid state entropies, elucidated by TLS analyses of the non-hydrogen ADPs. These results were later confirmed in a more elaborate multi-temperature study [105], where the hydrogen bond energies derived from topological analysis described in Sect. 5.3 are critically discussed as a method of determining the relative stabilities of closely related structures, such as enantiomeric compounds or polymorphs.

Charge density studies including disordered groups: In a recent 85 K X-ray charge density study of paracetamol, Bak and coworkers [106] examine different ways of modeling the disordered methyl group (Fig. 7). In this context, estimated hydrogen ADPs from the SHADE program seemed to offer advantages as compared to the ADPs based on neutron diffraction, partly because of the low quality of

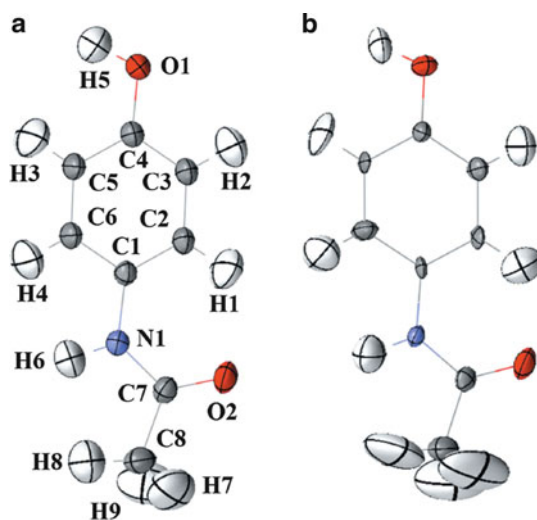


Fig. 7 Structure of paracetamol: (a) anisotropic displacement parameters (ADPs) at the 90% probability level for non-H atoms after high-order refinement against X-ray diffraction data (85 K) and for H atoms generated by the SHADE program; (b) ADPs at the 90% probability level from neutron diffraction data (80 K; [27])

the neutron diffraction data, and partly because of the disordered methyl groups, which seem to be easier to model using estimated ADPs. The application of ADPs taken from neutron experiments to the methyl H atoms led to extremely high values of electron density at the bond critical points. In the ordered part of the molecule, the use of ADPs generated by SHADE led to better residual maps derived from charge-density models than the neutron ADPs. We note that the other procedures for estimating H ADPs mentioned here (ADPH and TLS+ONIOM) would have been just as efficient as SHADE in this study. This study emphasizes the need to carefully consider the quality of the data. Even when a neutron diffraction dataset is available, it is mandatory to test its validity in every possible way. A high-quality neutron diffraction data set, where the disordered methyl group was carefully modeled using partially occupied sites, would probably have given the most physically reasonable results. Lacking such data, estimated ADPs seem to offer advantages as compared to a mediocre neutron diffraction dataset. A model using isotropic displacement parameters for hydrogen lead to extreme values for molecular electrostatic interaction energies, yet another confirmation that the isotropic model is insufficient for accurate charge density studies.

5 Outlook

Despite the fact that it is now more than three decades since Hirshfeld proposed a method to estimate the anisotropic motion of hydrogen atoms for the use in experimental charge-density analysis, it is only within the last years that the charge-density community at large has become familiar with the method – and with the model defects caused by omitting a careful treatment of the hydrogen atoms. Hopefully, this familiarity has raised general awareness that the description of the static charge density (in terms of the multipole model) and the description of atomic motion (in terms atomic anisotropic motion) are the ying and yang of charge density analysis – both aspects of the model has to be treated carefully, or both will be erroneous. The examples given in the last part of this chapter all reflect an awareness of the coupling between dynamic and static effects with careful treatment of both aspects.

Several tools are now available to estimate the hydrogen ADPs. We have discussed the merits of each of them – as well as advocating the use of neutron diffraction experiments whenever that is possible. However, whereas there seems to be a growing consensus regarding the treatment of nuclear positions and thermal motion for hydrogen, the flexibility of the multipole model of hydrogen is still debated, not only in terms of the truncation of the multipole expansion but also in terms of the flexibility of the radial parameters.

Ab initio calculations have been compared with static charge densities for several years. Looking ahead, the moment seems ripe to compare the dynamics of atoms and molecules obtained from ab initio calculations with the information from careful diffraction experiments.

References

1. Jeffrey GA (1997) An introduction to hydrogen bonding. Oxford University Press, Oxford
2. Munshi P, Madsen AØ, Spackman MA, Larsen S, Destro R (2008) Estimated H-atom anisotropic displacement parameters: a comparison between different methods and with neutron diffraction results. *Acta Crystallogr A* 64(4):465–475
3. Willis BTM, Pryor AW (1975) Thermal vibrations in crystallography. Cambridge University Press, Cambridge
4. Trueblood KN, Bürgi HB, Burzlaff H, Dunitz J, Gramaccioli CM, Schulz HH, Shmueli U, Abrahams SC (1996) Atomic displacement parameter nomenclature. Report of a subcommittee on atomic displacement parameter nomenclature. *Acta Crystallogr A* 52(5):770–781
5. Stewart RF, Davidson ER, Simpson WT (1965) Coherent X-ray scattering for the hydrogen atom in the hydrogen molecule. *J Chem Phys* 42(9):3175–3187
6. Chandler GS, Spackman MA (1982) Pseudoatom expansions of the first-row diatomic hydride electron densities. *Acta Crystallogr A* 38:225–239
7. Netzel J, Hofman A, van Smaalen S (2008) Accurate charge density of α -glycine by the maximum entropy method. *Cryst Eng Comm* 10:335–343
8. Netzel J, van Smaalen S (2009) Topological properties of hydrogen bonds and covalent bonds from charge densities obtained by the maximum entropy method (MEM). *Acta Crystallogr B* 65:624–638
9. Dietrich H (1976) ‘Core electrons’ of bonded hydrogen atoms. *Acta Crystallogr A* 32:347–348
10. Madsen AØ, Sørensen HO, Stewart RF, Flensburg C, Larsen S (2004) Modeling of nuclear parameters for hydrogen atoms in X-ray charge density studies. *Acta Crystallogr A* 60:550–561
11. Madsen AØ, Mason S, Larsen S (2003) A neutron diffraction study of xylitol: derivation of mean square internal vibrations for hydrogen atoms from a rigid-body description. *Acta Crystallogr B* 59:653–663
12. Birkedal H, Madsen D, Mathiesen RH, Knudsen K, Weber HP, Pattison P, Schwarzenbach D (2004) The charge density of urea from synchrotron diffraction data. *Acta Crystallogr A* 60(5):371–381
13. Flensburg C, Larsen S, Stewart RF (1995) Experimental charge density study of methylammonium hydrogen succinate monohydrate. A salt with a very short O–H–O hydrogen bond. *J Phys Chem* 99(25):10130–10141
14. Madsen D, Flensburg C, Larsen S (1998) Properties of the experimental crystal charge density of methylammonium hydrogen maleate. A salt with a very short intramolecular O–H–O hydrogen bond. *J Phys Chem A* 102(12):2177–2188
15. Whitten A, Spackman M (2006) Anisotropic displacement parameters for H atoms using an ONIOM approach. *Acta Cryst* 62:875–888. doi:10.1107/S0108768106020787, pp 1–14
16. Bader R (1994) Atoms in molecules. Oxford University Press, Oxford
17. Hoser AA, Dominiak PM, Wozniak K (2009) Towards the best model for H atoms in experimental charge-density refinement. *Acta Crystallogr A* 65(4):300–311
18. Roversi P, Destro R (2004) Approximate anisotropic displacement parameters for H atoms in molecular crystals. *Chem Phys Lett* 386:472–478
19. Roversi P, Barzaghi M, Merati F, Destro R (1996) Charge density in crystalline citrinin from X-ray diffraction at 19 K. *Can J Chem* 74:1145–1161
20. Bürgi HB, Capelli SC, Goeta AE, Howard JAK, Spackman MA, Yufit DS (2002) Electron distribution and molecular motion in crystalline benzene: an accurate experimental study combining CCD X-ray data on C_6H_6 with multitemperature neutron-diffraction results on C_6H_6 . *Chem A Eur J* 8(15):3512–3521
21. Mata I, Espinosa E, Molins E, Veintemillas S, Maniukiewicz W, Lecomte C, Cousson A, Paulus W (2006) Contributions to the application of the transferability principle and the

- multipolar modeling of H atoms: electron-density study of L-histidinium dihydrogen orthophosphate orthophosphoric acid. I. *Acta Crystallogr A* 62(5):365–378
22. Rousseau B, Maes ST, Lenstra ATH (2000) Systematic intensity errors and model imperfection as the consequence of spectral truncation. *Acta Crystallogr A* 56:300–307
23. Becker PJ, Coppens P (1975) Extinction within the limit of validity of the Darwin transfer equations. I. General formalisms for primary and secondary extinction and their application to spherical crystals. *Acta Crystallogr A* 31:129–147
24. Becker PJ, Coppens P (1975) Extinction within the limit of validity of the Darwin transfer equations. III. Non-spherical crystals and anisotropy of extinction. *Acta Crystallogr A* 31:417
25. Morgenroth W, Overgaard J, Clausen HF, Svendsen H, Jørgensen MRV, Larsen FK, Iversen BB (2008) Helium cryostat synchrotron charge densities determined using a large CCD detector – the upgraded beamline D3 at DESY. *J Appl Cryst* 41(5):846–853
26. Blessing RH (1995) On the differences between X-ray and neutron thermal vibration parameters. *Acta Crystallogr B* 51:816–823
27. Wilson C (2000) Single crystal neutron diffraction from molecular materials. World Scientific, Singapore
28. Kuhs WF (2003) International tables for crystallography. Kluwer Academic, Dordrecht, pp 228–242
29. Kuhs WF (1992) Generalized atomic displacements in crystallographic structure analysis. *Acta Crystallogr A* 48:80–98
30. Ruysink AFJ, Vos A (1974) Systematic errors in structure models obtained by X-ray diffraction. *Acta Crystallogr A* 30(4):503–506
31. Coppens P (1968) Evidence for systematic errors in X-ray temperature parameters resulting from bonding effects. *Acta Crystallogr B* 24(9):1272–1274
32. Hope H, Ottersen T (1978) Accurate determination of hydrogen positions from X-ray data. I. The structure of s-diformohydrazide at 85 K. *Acta Crystallogr B* 34:3623–3626
33. Almlöf J, Otterson T (1979) X-ray high-order refinements of hydrogen atoms: a theoretical approach. *Acta Crystallogr A* 35:137–139
34. Stewart RF, Bentley J, Goodman B (1975) Generalized x-ray scattering factors in diatomic molecules. *J Chem Phys* 63(9):3786–3793
35. Stewart RF, Spackman M, Flensburg C (1998) VALRAY98 users manual
36. Destro R, Marsh R, Bianchi R (1988) A low-temperature (23-K) study Of L-alanine. *J Phys Chem* 92(4):966–973
37. Destro R, Roversi P, Barzaghi M, Marsh RE (2000) Experimental charge density of α -Glycine at 23 K. *J Phys Chem A* 104:1047–1054
38. Destro R, Soave R, Barzaghi M, Lo Presti L (2005) Progress in the understanding of drug-receptor interactions, Part 1: experimental charge-density study of an angiotensin II receptor antagonist (C30H30N6O3S) at T=17 K. *Chem A Eur J* 11(16):4621–4634
39. Allen FH, Watson DG, Brammer L, Orpen AG, Taylor R (1999) Typical interatomic distances: organic compounds. In: Wilson AJC, Prince E (eds) International tables for crystallography. Kluwer Academic, Dordrecht, pp 782–803
40. Overgaard J, Platts JA, Iversen BB (2009) Experimental and theoretical charge-density study of a tetranuclear cobalt carbonyl complex. *Acta Crystallogr B* 65(6):715–723
41. Steiner T, Saenger W (1994) Lengthening of the covalent O-H bond in O-H...O hydrogen bonds re-examined from low-temperature neutron diffraction data of organic compounds. *Acta Crystallogr B* 50:348–357
42. Jayatilaka D, Dittrich B (2008) X-ray structure refinement using aspherical atomic density functions obtained from quantum-mechanical calculations. *Acta Crystallogr A* 64 (Pt 3):383–393
43. Hirshfeld F (1977) Bonded-atom fragments for describing molecular charge-densities. *Theor Chim Acta* 44(2):129–138
44. Harel M, Hirshfeld F (1975) Difference densities by least-squares refinement. II. Tetracyanocyclobutane. *Acta Crystallogr B* 31:162–172

45. Hirshfeld F (1976) Can X-ray data distinguish bonding effects from vibrational smearing? *Acta Crystallogr A* 32:239–244
46. Hirshfeld F, Hope H (1980) An X-ray determination of the charge deformation density in 2-cyanoguanidine. *Acta Crystallogr B* 36:406–415
47. Eisenstein M, Hirshfeld F (1983) Experimental versus theoretical charge densities: a hydrogen-bonded derivative of bicyclobutane at 85 K. *Acta Crystallogr B* 39:61–75
48. Cruickshank DWJ (1956) The analysis of the anisotropic thermal motion of molecules in crystals. *Acta Crystallogr* 9:754
49. Schomaker V, Trueblood KN (1968) On the rigid-body motion of molecules in crystals. *Acta Crystallogr B* 24:63–76
50. Dunitz JD, Maverick EF, Trueblood KN (1988) Atomic motions in molecular crystals from diffraction measurements. *Angew Chem Int Ed Engl* 27:880–895
51. Dunitz JD (1978) X-ray analysis and the structure of organic molecules. Cornell University Press, Ithaca
52. Schomaker V, Trueblood KN (1998) Correlation of internal torsional motion with overall molecular motion in crystals. *Acta Crystallogr B* 54:507–514
53. Spek A (1990) PLATON, an integrated tool for the analysis of the results of a single crystal structure determination. *Acta Crystallogr A* 46:C34
54. He XM, Craven B (1985) Internal molecular vibrations from crystal diffraction data by quasinormal mode analysis. *Acta Crystallogr A* 41:244–251
55. He XM, Craven B (1993) Internal vibrations of a molecule consisting of rigid segments. I. Non-interacting internal vibrations. *Acta Crystallogr A* 49:10–22
56. Capelli S, Hauser J (2004) NKA user manual, 16th edn. Universität Bern
57. Burgi H, Capelli S (2000) Dynamics of molecules in crystals from multi-temperature anisotropic displacement parameters. I. Theory. *Acta Crystallogr A* 56:403–412
58. Capelli S, Förtsch M, Burgi H (2000) Dynamics of molecules in crystals from multi-temperature anisotropic displacement parameters. II. Application to benzene (C₆D₆) and urea [OC(NH)₂]. *Acta Crystallogr A* 56(5):413–424
59. Rosenfield RE Jr, Trueblood KN, Dunitz J (1978) A test for rigid-body vibrations, based on a generalization of Hirshfeld's 'rigid-bond' postulate. *Acta Crystallogr A* 34:828–829
60. Klooster W, Ruble J, Craven B, McMullan RK (1991) Structure and thermal vibrations of adenosine from neutron diffraction data at 123 K. *Acta Crystallogr B* 47(3):376–383
61. May E, Destro R, Gatti C (2001) The unexpected and large enhancement of the dipole moment in the 3,4-bis(dimethylamino)-3-cyclobutene-1,2-dione (DMACB) molecule upon crystallization: A new role of the intermolecular CH...O interactions. *J Am Chem Soc* 123(49):12248–12254
62. Forni A, Destro R (2003) Electron density investigation of a push-pull ethylene(C₁₄H₁₂NO₂ · H₂O) by x-ray diffraction at T=21 K. *Chem A Eur J* 9(22):5528–5537
63. Soave R, Barzaghi M, Destro R (2007) Progress in the understanding of drug-receptor interactions, part 2: experimental and theoretical electrostatic moments and interaction energies of an angiotensin II receptor antagonist (C₃₀H₃₀N₆O₃S). *Chem A Eur J* 13(24):6942–6956
64. Johnson CK (1970) Thermal neutron diffraction. Oxford University Press, Oxford
65. Weber HP, Craven B, Sawzip P, McMullan R (1991) Crystal structure and thermal vibrations of Cholesteryl Acetate from neutron diffraction at 123 and 20 K. *Acta Crystallogr B* 47:116–127
66. Gao Q, Weber HP, Craven B, McMullan R (1994) Structure of suberic acid at 18.4, 75 and 123 K from neutron diffraction data. *Acta Crystallogr B* 50(6):695–703
67. Kampermann SP, Sabine TM, Craven B, McMullan R (1995) Hexamethylenetetramine: extinction and thermal vibrations from neutron diffraction at six temperatures. *Acta Crystallogr A* 51:489–497. doi:[10.1107/S0108767394013711](https://doi.org/10.1107/S0108767394013711), pp 1–9
68. Luo J, Ruble J, Craven B, McMullan R (1996) Effects of H/D substitution on thermal vibrations in piperazinium hexanoate-H11, D11. *Acta Crystallogr B* 52(2):357–368

69. Trueblood KN, Dunitz JD (1983) Internal molecular motions in crystals. The estimation of force constants, frequencies and barriers from diffraction data. A feasibility study. *Acta Crystallogr B* 39:120–133
70. Madsen AØ (2006) SHADE web server for estimation of hydrogen anisotropic displacement parameters. *J Appl Crystallogr* 39:757–758
71. Hall SR, Allen FH, Brown ID (1991) The crystallographic information file (CIF): a new standard archive file for crystallography. *Acta Crystallogr A* 47:655–685
72. Koritsanszky T, Howard S, Mallinson P, Su Z, Richter T, Hansen NK (1996) XD: a computer program package for multipole refinement and analysis of electron densities from diffraction data, 1st edn
73. Frisch MJ, Trucks GW, Schlegel HB, Scuseria GE, Robb MA, Cheeseman JR, Montgomery Jr JA, Vreven T, Kudin KN, Burant JC, Millam JM, Iyengar SS, Tomasi J, Barone V, Mennucci B, Cossi M, Scalmani G, Rega N, Petersson GA, Nakatsuji H, Hada M, Ehara M, Toyota K, Fukuda R, Hasegawa J, Ishida M, Nakajima T, Honda Y, Kitao O, Nakai H, Klene M, Li X, Knox JE, Hratchian HP, Cross JB, Bakken V, Adamo C, Jaramillo J, Gomperts R, Stratmann RE, Yazyev O, Austin AJ, Cammi R, Pomelli C, Ochterski JW, Ayala PY, Morokuma K, Voth GA, Salvador P, Dannenberg JJ, Zakrzewski VG, Dapprich S, Daniels AD, Strain MC, Farkas O, Malick DK, Rabuck AD, Raghavachari K, Foresman JB, Ortiz JV, Cui Q, Baboul AG, Clifford S, Cioslowski J, Stefanov BB, Liu G, Liashenko A, Piskorz P, Komaromi I, Martin RL, Fox DJ, Keith T, Al-Laham MA, Peng CY, Nanayakkara A, Challacombe M, Gill PMW, Johnson B, Chen W, Wong MW, Gonzalez C, Pople JA (2003) Gaussian 03, Revision C.02. Tech. Rep., Gaussian, Inc., Wallingford, 2004
74. Flaig R, Koritsanszky T, Zobel D, Luger P (1998) Topological analysis of the experimental electron densities of amino acids. 1. D, L-aspartic acid at 20 K. *J Am Chem Soc* 120:2227–2238
75. Oddershede J, Larsen S (2004) Charge density study of naphthalene based on X-ray diffraction data at four different temperatures and theoretical calculations. *J Phys Chem A* 108:1057–1063
76. Whitten AE, Spackman MA (2006) Anisotropic displacement parameters for H atoms using an ONIOM approach. *Acta Crystallogr B* 62:875–888
77. Madsen AØ, Civalleri B, Pascale F, Dovesi R (2012) Anisotropic displacement parameters for molecular crystals from periodic HF and DFT calculations. *Acta Crystallogr A* (in press)
78. Scott AP, Radom L (1996) Harmonic vibrational frequencies: an evaluation of Hartree-Fock, Møller-Plesset, quadratic configuration interaction, density functional theory, and semiempirical scale factors. *J Phys Chem* 100:16502–16513
79. Born M, Huang K (1954) Dynamical theory of crystal lattices. Clarendon, Oxford
80. Filippini G, Gramaccioli CM, Simonetta M, Suffritti BG (1974) On some problems connected with thermal motion in molecular crystals and a lattice-dynamical interpretation. *Acta Crystallogr A* 30:189–196
81. Gramaccioli CM, Filippini G (1983) Lattice-dynamical evaluation of temperature factors in non-rigid molecular crystals: a first application to aromatic hydrocarbons. *Acta Crystallogr A* 39:784–791
82. Gramaccioli CM, Filippini G, Simonetta M (1982) Lattice-dynamical evaluation of temperature factors for aromatic hydrocarbons, including internal molecular motion: a straightforward systematic procedure. *Acta Crystallogr A* 38:350–356
83. Criado A (1990) Lattice dynamics and thermal parameters in azahydrocarbons. *Acta Crystallogr A* 46:489–494
84. Willis BTM, Howard J (1975) Do the ellipsoids of thermal vibration mean anything? – analysis of neutron diffraction measurements on hexamethylenetetramine. *Acta Crystallogr A* 31:514–520
85. Flensburg C, Stewart RF (1999) Lattice dynamical Debye-Waller factor for silicon. *Phys Rev* 60(1):284–290

86. Parlinski K, Li ZQ, Kawazoe Y (1997) First-principles determination of the soft mode in Cubic ZrO₂. *Phys Rev Lett* 78(21):4063–4066
87. Lee C, Gonze X (1995) Ab initio calculation of the thermodynamic properties and atomic temperature factors of SiO₂ α -quartz and stishovite. *Phys Rev B* 51(13):8610–8613
88. Langkilde A, Kristensen SM, Lo Leggio L, Molgaard A, Jensen JH, Houk AR, Poulsen JCN, Kauppinen S, Larsen S (2008) Short strong hydrogen bonds in proteins: a case study of rhamnogalacturonan acetyltransferase. *Acta Crystallogr D Biol Crystallogr* 64(Pt 8):851–863
89. Madsen G, Iversen B, Larsen F, Kapon M, Reisner G, Herbststein F (1998) Topological analysis of the charge density in short intramolecular O–H · hydrogen bonds. Very low temperature X-ray and neutron diffraction study of benzoylacetone. *J Am Chem Soc* 120(13):10040–10045
90. Schmidtmann M, Farrugia LJ, Middlemiss DS, Gutmann MJ, McIntyre GJ, Wilson CC (2009) Experimental and theoretical charge density study of polymorphic isonicotinamide-oxalic acid molecular complexes with strong O · N hydrogen bonds. *J Phys Chem A* 113(50):13985–13997
91. Brown AS, Spackman M (1994) The determination of electric-field gradients from X-Ray-diffraction data. *Mol Phys* 83(3):551–566
92. Fournier B, Bendeif EE, Guillot B, Podjarny A, Lecomte C, Jelsch C (2009) Charge density and electrostatic interactions of fidarestat, an inhibitor of human aldose reductase. *J Am Chem Soc* 131:10929–10941
93. Johnson CK (1976) ORTEP. Report ORNL-5138. Tech. Rep., Tennessee
94. Delano WL (2006) The PyMOL molecular graphics system. Tech. Rep., Delano Scientific, San Carlos
95. Spackman M, Byron PG, Alfredsson M, Hermansson K (1999) Influence of intermolecular interactions on multipole-refined electron densities. *Acta Crystallogr A* 55:30–47
96. de Vries RY, Feil D, Tsirelson VG (2000) Extracting charge density distributions from diffraction data: a model study on urea. *Acta Crystallogr B* 56:118–123
97. Saunders VR, Dovesi R, Roetti C, Causa M, Harrison NM, Orlando R, Zicovich-Wilson CM (1998) Crystal 98 users manual
98. Dittrich B, Spackman M (2007) Can the interaction density be measured? The example of the non-standard amino acid sarcosine. *Acta Crystallogr A* 63(Pt 5):426–436
99. Espinosa E, Molins E, Lecomte C (1998) Hydrogen bond strengths revealed by topological analyses of experimentally observed electron densities. *Chem Phys Lett* 285:170–173
100. Espinosa E, Souhassou M, Lachekar H, Lecomte C (1999) Topological analysis of the electron density in hydrogen bonds. *Acta Crystallogr B* 55:563–572
101. Espinosa E, Lecomte C, Molins E (1999) Experimental electron density overlapping in hydrogen bonds: topology vs. energetics. *J Chem Phys* 300:745–748
102. Mata I, Espinosa E, Molins E, Veintemillas S, Maniukiewicz W, Lecomte C, Cousson A, Paulus W (2006) Contributions to the application of the transferability principle and the multipolar modeling of H atoms: electron-density study of l-histidinium dihydrogen orthophosphate orthophosphoric acid. I *Acta Crystallogr A* 62:365–378. doi:[10.1107/S0108767306025141](https://doi.org/10.1107/S0108767306025141), pp 1–14
103. Espinosa E, Alkorta I, Elguero J, Molins E (2002) From weak to strong interactions: a comprehensive analysis of the topological and energetic properties of the electron density distribution involving X–H ··· F–Y systems. *J Chem Phys* 117(12):5529–5542
104. Madsen AØ, Larsen S (2007) Insights into solid state thermodynamics from diffraction data. *Angew Chemie Int Ed Engl* 46:8609–8613
105. Madsen AØ, Mattson R, Larsen S (2011) Understanding thermodynamic properties at the molecular level: multiple temperature charge density study of ribitol and xylitol. *J Phys Chem A* 115(26):7794–7804
106. Bak J, Dominiak P, Wilson C, Wozniak K (2009) Experimental charge-density study of paracetamol – multipole refinement in the presence of a disordered methyl group. *Acta Crystallogr A* 65:490–500. doi:[10.1107/S0108767309031729](https://doi.org/10.1107/S0108767309031729), pp 1–11

<http://www.springer.com/978-3-642-30801-7>

Electron Density and Chemical Bonding I

Experimental Charge Density Studies

Stalke, D. (Ed.)

2012, XII, 212 p., Hardcover

ISBN: 978-3-642-30801-7